Retardation of ice growth in glass capillaries: Measurement of the critical capillary radius

Zhihong Liu,[1] Ken Muldrew,[2,*] Richard G. Wan,[1] and Janet A. W. Elliott[3]
[1]*Department of Civil Engineering, University of Calgary, Calgary, Alberta, Canada T2N 1N4*
[2]*Department of Cell Biology and Anatomy, University of Calgary, Calgary, Alberta, Canada T2N 4N1*
[3]*Department of Chemical and Materials Engineering, University of Alberta, Edmonton, Alberta, Canada T6G 2G6*
(Received 2 September 2003; published 27 February 2004)

An experiment was designed to compare the freezing of an aqueous solution in glass microcapillaries and in thin films. The velocity dependence of the ice front propagation in glass capillaries with radii of 87.5 μm–1.5 μm was observed. A critical capillary radius r_0, corresponding to certain thermal conditions, was obtained, below which the ice growth inside the capillaries was retarded. This critical capillary radius is further related to λ_0, the smallest wavelength used in the Mullins-Sekerka criterion for the instability analysis of bulk solidifications [Mullins and Sekerka, J. Appl. Phys. **35**, 444 (1964)]. It was found that for the present hypothesis, $r_0=\lambda_0/4$ gives good predictions. The relation between the propagation velocity (or cooling rate) and the critical radius (or pore size) is summarized in a chart for applications in capillary-porous media, such as in the freezing of biological tissues.

DOI: 10.1103/PhysRevE.69.021611 PACS number(s): 68.08.−p, 47.20.Hw, 81.30.Fb, 87.10.+e

I. INTRODUCTION

Ice growth in an aqueous solution is generally limited by three factors: (1) the diffusion of heat and solute away from the ice-solution interface; (2) the interfacial tension between the ice and the solution; and (3) the kinetics of attachment of water molecules to the ice surface [1]. The competition of these factors determines whether the growth is stable or unstable and how fast the growth is. The third factor, usually referred to as ''kinetic supercooling'' [2], will not be discussed in the present paper, given that the cooling rate is not high enough to bring a significant effect of kinetic supercooling in the conventional freezing of soils and/or biological tissues, which are the primary concerns to be addressed herein.

The diffusion processes are driven by the gradients in temperature or concentration. As the solute is excluded from the newly formed solid phase, it forms a mass boundary layer in the liquid near the interface. Because of the increased concentration and concentration gradient, the diffusion of solute in this boundary layer gets faster. Once the rate of mass diffusion overrides the rate of latent heat removal (through ice, the temperature gradient has been assumed ''positive'' near the interface), the boundary layer solution becomes supercooled (i.e., ''constitutional supercooling'' [3]). A supercooled solution is metastable, and unstable (''cellular'' or ''dendritic'') ice growth can be readily initiated if the interfacial tension effect is minor. Once perturbed, the interface will alter the concentration distribution in the liquid, leaving the solute more concentrated between ''ice fingers.'' This leads to a more efficient diffusion mode for the solute (usually in a higher two-dimensional or three-dimensional manner) and more constitutional supercooling in the liquid as well. The unstable growth of ice in such a positive temperature gradient is called ''constrained growth'' [1], since the growth of ice structures is constrained by the rate of the advance of *isotherms*. This is the normal situation of unidirectional solidification in *bulk* solutions.

Capillarity plays a role when solidification occurs in small, narrow spaces, such as in microcapillaries or within a capillary-porous medium [4,5]. Capillarity refers to the large ratio of the interfacial free energies, between the ice, the solution, and the capillary wall, to the volume energy; besides, heat and mass transfer at microscales is also constrained, and significantly influenced by the morphology of the growing boundary between the solid and the liquid [6,7]. At certain circumstances, the size of new crystal to be formed is so small that the latent heat released from the volume of ice to undergo the phase transformation might not allow a new interface to initiate unstable growth. In this situation, the original solute diffusion mode, essentially one dimensional in the ice growth direction, cannot be altered (even though the liquid is supercooled). The ice growth is then limited by the diffusion of *solute* in the direction of thermal gradient, which is much slower.

A question of fundamental interest in both civil and biomedical engineering is to characterize the critical size (or more precisely the critical conditions) under which unstable growth will not be developed in small capillaries or capillary-porous systems. One of the motivating factors for pursuing this line of inquiry is the intriguing case of freezing articular cartilage. Articular cartilage is the tissue that is located at the end of the long bones, distributing load between the bones and providing a near-frictionless surface for articulation. Unfortunately, all attempts to cryopreserve articular cartilage for transplantation have failed to keep the cartilage viable. Research work that attempted to scale cryopreservation techniques for isolated chondrocytes (usually preserved in solutions) to the intact tissue met with poor results, leading to questions about whether the structure of the tissue was affecting the ice growth [8–11]. A recent scanning electron micrograph investigation of frozen cartilage samples suggested that, unlike the freezing of cell suspensions in bulk, cellular or dendritic ice growth was seldom observed in the freezing of this tissue [9]. Muldrew *et al.* further hypoth-

*Electronic address: kmuldrew@ucalgary.ca

esized that the pore size of the cartilage tissue (≈5 nm [12]) is not large enough to allow cellular or dendritic growth so that the ice front would appear, macroscopically, as a planar front and remain ''planar'' even at very low temperatures.

In the cryobiological context, ice formation within muscle fibers was investigated by Rapatz and Luyet (1966) [13]. They observed that as ice progresses in the longitudinal direction of the muscle fibers, spears increase in thickness, separating and pushing aside the solid constituents of the fibers. Development of protuberances on the spears was also shown in their pictures. However, the diameters of the muscle fibers they examined were about 30–50 μm, which could be too large to demonstrate an obvious capillary effect for the solidification of aqueous solutions.

A thin, quasi-two-dimensional sample layer (≈10 μm in thickness) of a binary aqueous solution (sodium permanganate) was studied by Körber and Scheiwe (1983) [14] for the nonplanar solidification. They used a light microscope equipped with a freezing stage and a spectrophotometer to measure solute redistribution and concentration profiles along the interdendritic midlines. The instability criterion was validated with respect to the constitutional supercooling. The capillary effect, however, was not demonstrated through the experimental setup, since one of the dimensions perpendicular to the ice growth direction was still bulk: the width of the samples was about 2000–3000 μm.

This paper will present a freezing experiment that can explore the dimensional dependence of ice fronts propagating in small containers: (1) thin films and (2) capillaries. To simulate as closely as possible the real temperature profile in freezing tissue volumes, a nearly parabolic temperature distribution (lower outside and higher inside) was applied to the experimental system through a customized conduction cryostage. Since the temperature profile has a positive temperature gradient at the interface, it can supply the ''constrained growth'' condition for bulk solutions. The velocity of the ice fronts was measured with the traveling cryostage and a video camera. A critical capillary radius r_0 corresponding to certain thermal conditions will be examined below which ice growth inside the restricted volume is retarded. In Sec. III, the Mullins-Sekerka criterion for interface instability that was originally documented in metallurgical solidification (for bulk solutions or alloys) [15], will be introduced and tailored to the study of this interesting phenomenon. This work is expected to give some insight toward understanding the freezing of biological tissues, a challenging problem.

II. EXPERIMENT

Two independent experiments were performed in parallel with an aqueous solution of potassium permanganate (Sigma Chemical Co., MO, US). One experiment investigated the freezing of a thin film of solution that was trapped between two glass slides while the other experiment focused on the solidification of solution within glass capillary tubes (Fig. 1). Both experiments were subjected to the same freezing protocol. The only difference between the two experiments was the dimension of solution samples in the plane perpendicular to the growth direction (i.e., x axis). For the film samples,

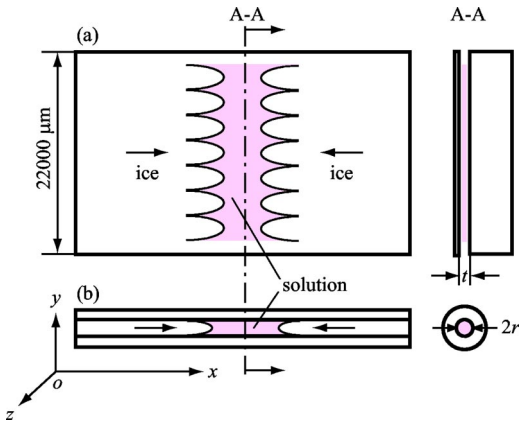

FIG. 1. Two independent freezing experiments are performed with respect to (a) solution film; (b) solution in capillary. The transient positions of ice front tips are recorded with a video camera.

their size in the y direction was ''unconstrained'' and could be as much as 22 000 μm. Both the thickness of the films (t) and the diameter of capillaries ($D=2r$) were varied from a high value (≈175 μm) to a low value (≈3 μm) during the experiments. Transient positions of the ice front tips were recorded in both cases by the video camera to determine the velocity dependence upon the dimensions of the solution to be frozen.

A. Experimental apparatus

As shown in Fig. 2, a customized cryostage has been manufactured and mounted on a light microscope (Zeiss, Germany), which is readily equipped with a charge-coupled device video camera (JVC TK-1070U) and a video recording system (Hitachi M250A Video Recorder). The x and y positions of the cryostage are controlled, by moving the platform of the microscope, so that the ice fronts are maintained at the center of view. The cryostage is a conduction type and consists of two copper bases. They are enclosed in a circular acrylic box, separated by a 10 mm air gap and bridged with a glass slide ($60\times25\times1$ mm^3). The copper bases, both having a hole inside, are hooked up in series with vinyl tubing (1/4-in.-ID, not shown in the figure) through two hydraulic connectors (Swagelok 1/4-in.-hose size, Calgary, Canada) on

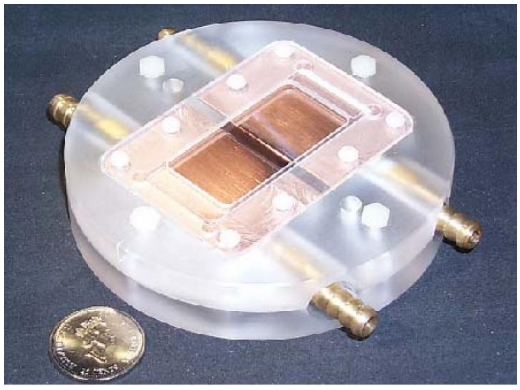

FIG. 2. A customized conduction cryostage (a quarter coin at the left-bottom corner is for size comparison).

the left side of the stage; the other two connectors on the right side are connected to an alcohol cooling bath (FP 40, Julabo, Germany) to form a circulation loop. The open rectangular window at the center of the box was left for sample mounting.

The temperature of the glass slide $\theta(x)$ varies from edge to edge. It reaches the maximum at the midpoint ($x=5$ mm) and has a symmetric distribution that ensures a convenient comparison of experimental data from both edges. The thermal system, to a first-order approximation, can be described by a quasistationary, one-dimensional model of heat conduction in a glass slab cooled at the surfaces by convection [16,17]. The temperature across the gap ($d=10$ mm) is given by the following equation:

$$\frac{d^2T}{d\xi^2}=\psi^2T, \tag{1}$$

where $T=\theta-\theta_{\text{air}}$, $\xi=x/d$, and $\psi=d\sqrt{2h/t_{\text{slide}}k_{\text{slide}}}$. Basically, $\theta_{\text{air}}=20\,^{\circ}\text{C}$ is the ambient temperature; $t_{\text{slide}}=1$ mm is the thickness of the glass slide; $h\approx 4-8$ J/(sec m^2 K) is heat transfer coefficient of air (natural convection), and $k_{\text{slide}}=1.3$ J/(sec m K) is the thermal conductivity of glass. The solution to Eq. (1) is

$$T(x)=A[e^{\psi(x/d)}+e^{\psi(1-(x/d))}], \tag{2}$$

and

$$A=\frac{T_{\text{edges}}+\sqrt{T_{\text{edges}}^2-T_{\text{midline}}^2}}{2}, \tag{3a}$$

$$\psi=2\ln\tan\frac{\pi-\arcsin\dfrac{T_{\text{midline}}}{T_{\text{edges}}}}{2}, \tag{3b}$$

where $T_{\text{edges}}=\theta_{\text{edges}}-\theta_{\text{air}}$, $T_{\text{midline}}=\theta_{\text{midline}}-\theta_{\text{air}}$; and θ_{edges} and θ_{midline} are the transient temperatures at the edges and midline of the gap, to be measured by thermocouples in real time, respectively (details will be discussed in the following).

Equation (2) will be used to estimate the transient temperature gradient G near the interface as well when ice growth becomes unstable, i.e.,

$$G(x)=\frac{\partial\theta}{\partial x}=\frac{\partial T}{\partial x}=\frac{\psi}{d}A[e^{\psi(x/d)}-e^{\psi(1-(x/d))}]. \tag{4}$$

The bottom surface of the glass slide within the 10 mm gap between the copper bases was divided previously by 11 lines parallel to the base edges with a ''Sanford'' permanent marker. The lines were evenly distributed at an interval of 1 mm for conveniently locating the ice fronts during the experiment. When the ice front tips passed through the marks or the middle lines between two neighboring marks, time was measured using a stopwatch (VWR, Control Company, China).

The freezing protocol was programmed through the bath controller (Table I). It consisted of four segments each segment being defined by two parameters: one being the end temperature (θ_{bath}) and the other being the time duration (Δt) that the bath will take to reach the end temperature. Before executing any freezing protocol, the alcohol bath was preset to $-3\,^{\circ}$C. The Julabo FP40 can control the temperature of the coolant within an error band of $\pm 0.5\,^{\circ}$C. However, due to the thermal damping of the coolant and the stage, the resultant temperature on the glass slide was higher than the programmed value and usually was delayed about 150 sec for the current experimental setup. The transient temperatures on the slide at the left edge (0 mm mark) and the midline of the gap (5 mm mark) were measured by a pair of *T*-type thermocouples (Precision fine wire, 0.001 Ga., Omega Engineering, Inc., CT, US). The data were recorded in Fig. 3 and fitted with the ramped temperature profile given in Table I for further analysis. After processing of the data, it was found that $T_{\text{midline}}/T_{\text{edges}}$ is almost constant (≈ 0.90), which yields $\psi\approx 0.93$. This result is consistent with the alternative calculation based on $\psi=d\sqrt{2h/t_{\text{slide}}k_{\text{slide}}}$.

TABLE I. Freezing protocol and the real temperatures on the glass slide.

Segment no.	θ_{bath} (°C)	Δt (min)	θ_{edges} (°C)	θ_{midline} (°C)	Δt (min)
1	−3	0	−0.3	2.0	2.5
2	−10	14	−5.5	−2.5	14
3	−3	14	−0.3	2.0	14
4	−3	5	−0.3	2.0	2.5

B. Materials and methods

The potassium permanganate solution (16 mOsm) was prepared and calibrated by a standard Osmometer (Precision

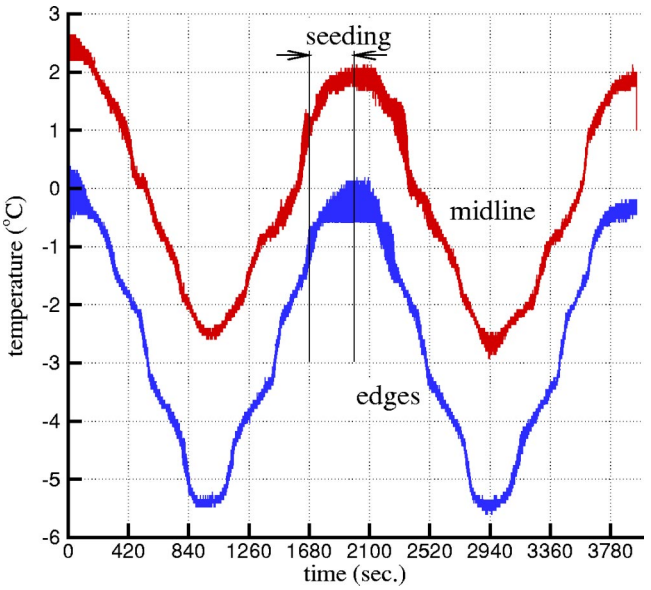

FIG. 3. The measured temperature-time profiles at the edges and the midline of the 10 mm glass slide span, respectively. Two repeats of the freezing protocol were recorded with an interval of 5 min for ice seeding.

Systems Inc., MA, US). The freezing point for this dilute solution is $\theta_0 \approx -0.03\,^{\circ}\mathrm{C}$.

1. Solution in thin films

The solution was placed on the glass slide of the cryostage and covered by a 22×22 mm^2 cover slip. Due to the effect of capillary suction, the liquid droplet filled immediately the space between the two glass surfaces and formed a thin layer of the liquid. The thickness of the liquid layer can be conveniently varied, by controlling the volume to be added, via an adjustable pipette (0, 5–10 μL, Eppendorf, Hamburg, Germany). As the liquid volume is decreased from 10 μL to 2 μL, the corresponding thickness of the solution layer is decreased, proportionally, from 20 μm to 4 μm. Note that 2 μL is the minimum volume of solution that we could use in the experiment, in order to maintain a uniform thickness of the film without introducing a large amount of air bubbles.

2. Solution in capillaries

Microcapillaries were pulled from a micropipette (5 μL, Fisher Scientific, Canada). Before pulling, the micropipette was carefully cleaned to remove oil or dust inside. The details of the pulling and cleaning procedures can be found in a previous paper [18]. Once pulled, the glass capillaries were cut to 35 mm long and filled with the binary solution by capillary suction. They were then placed on the glass slide parallel to the longitudinal axis. A layer of alginate gel was spread over the capillaries to enhance heat transfer. A glass cover slip (22×22 mm^2) was then put on the top of the alginate gel for heat insulation and optical observation. The alginate gel was previously mixed with a small amount of certified latex beads (20 μm, Coulter Electronics, Inc., FL, US). These transparent silica beads, with an almost uniform size, were used for calibrating distance; e.g., to determine the diameters of the capillaries.

As the temperature of the cooling bath was lowered to $-3\,^{\circ}\mathrm{C}$, at which temperature the bath was held for 5 min, ice was seeded by touching dry ice to both edges of the cryostage or to both ends of the capillaries. After ice was nucleated, the open window was covered by another cover slide for further heat insulation to prevent vapor condensation during the freezing. Once the bath temperature began to drop down from $-3\,^{\circ}\mathrm{C}$, the VCR was started for event recording, until the freezing cycle was completed.

C. Results

As the temperature was further lowered, the ice fronts were observed to start propagating, parallel to the longitudinal direction of the slide, from both sides of the gap (i.e., at the 0 mm and 10 mm marks) and advance simultaneously towards the midline (i.e., the 5 mm mark).

Transition of the planar ice fronts to the nonplanar form took place at about 180 sec for the thin films of the solution, as the fronts passed through the ''1 mm'' and ''9 mm'' marks, respectively. Due to the symmetry of the thermal system, only half of the slide is discussed in the following. The transition corresponded to a local temperature, $\theta(x^*) \approx -0.5\,^{\circ}\mathrm{C}$; and a local temperature gradient, $G(x^*) \approx 0.7$ K/mm at the interface, where $x^* = 1$ mm is the coordinate of the planar/nonplanar transition point. From this point on, the ice fronts were no longer straight. The event then involved the evolution of two groups of ''ice fingers'' until they merged at the 5 mm mark.

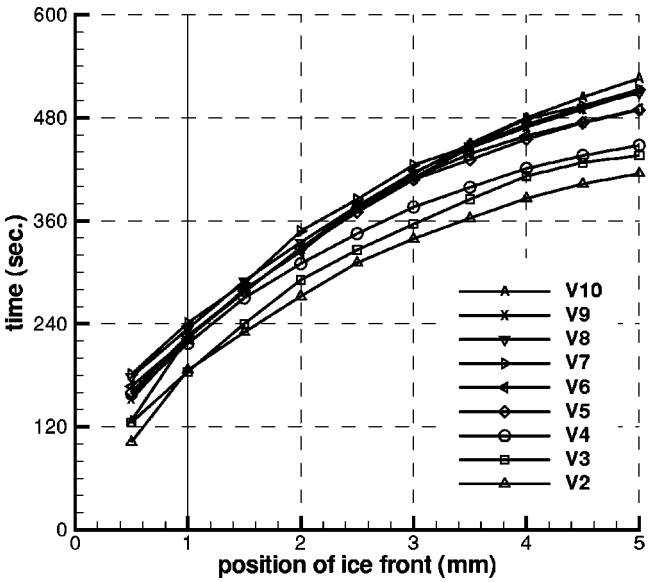

FIG. 4. The transient position of ice front tips vs time for film freezing (case 1, $\Delta t = 14$ min). The volume of the sample solution is indicated in μL following the letter ''V.''

The averaged transient position of the ice front tips was recorded and plotted against time in Fig. 4. As we have mentioned before, the thickness of the films was controlled by adjusting the volume of solution to be added to the slide. As the film thickness drops from 20 μm (''V10'') to 4 μm (''V2''), the shape of the position-time profiles does not change much, though the curves themselves are displaced in the time direction.

Figure 5 shows the position-time profiles for the capillary freezing. As the capillary diameters were decreased from 175 μm to 14 μm, the shape of the position-time profiles were also displaced in the time direction, in a similar manner as we have observed in Fig. 4. The ice growth starting at different intervals could be due to the fact that for larger diameters of capillaries, a larger amount of heat needs to be removed during freezing, which delays the ice growth.

In contrast to Fig. 4, the position-time profiles in Fig. 5, however, began to ''spring back'' as the capillary size kept decreasing from 14 μm to 8 μm or 5 μm, and showed characteristics of their own: the growth rate was slowed. The critical diameter of capillaries in which ice growth became retarded, for this case, was about 14 μm; i.e., $r_0 \approx 7$ μm. Note that in the freezing of solution films (Fig. 4), we did not observe any retardation, even if the thickness of film had been as small as 4 μm. The reason for this difference will be discussed in the following section.

Figure 5 was superposed over Fig. 4, and we found that for either the film solution with a controlled volume greater than 2 μL, or the solution within a capillary of diameter larger than 14 μm, the position-time profiles actually over-

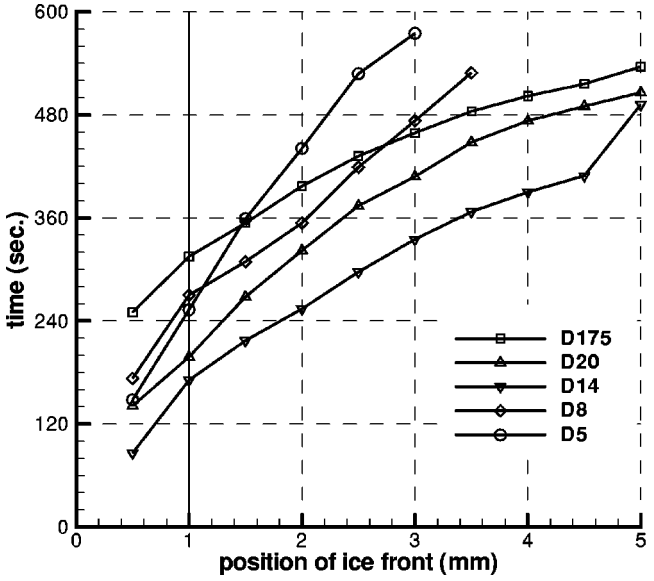

FIG. 5. The transient position of ice front tips vs time for capillary freezing (case 1, $\Delta t = 14$ min). The diameter of the capillary is indicated in μm following the letter "D."

lapped a lot and shared a similar shape. This is consistent with what we would expect for the so-called isotherm-constrained freezing of bulk solutions.

Additional experiments, with different cooling rates, have been performed by changing the freezing time duration (Δt) from the original 14 min to 21 min and 28 min, respectively (namely, case 2 and case 3). For the new cases, both film and capillary data were collected and plotted in a single figure for comparison, as illustrated in Figs. 6 and 7, respectively. Note that the experimental data for the films are indicated by

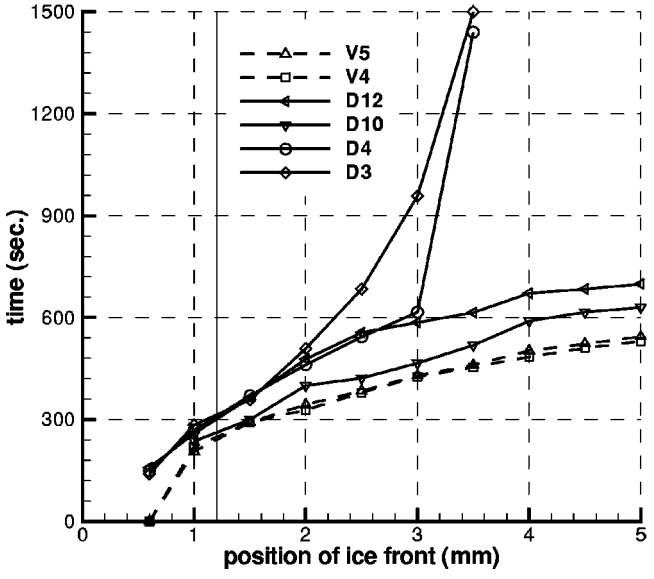

FIG. 6. The transient position of ice front tips vs time for both film and capillary freezing (case 2, $\Delta t = 21$ min). The volume of the film solution is indicated in μL following the letter "V"; the diameter of the capillary is indicated in μm following the letter "D."

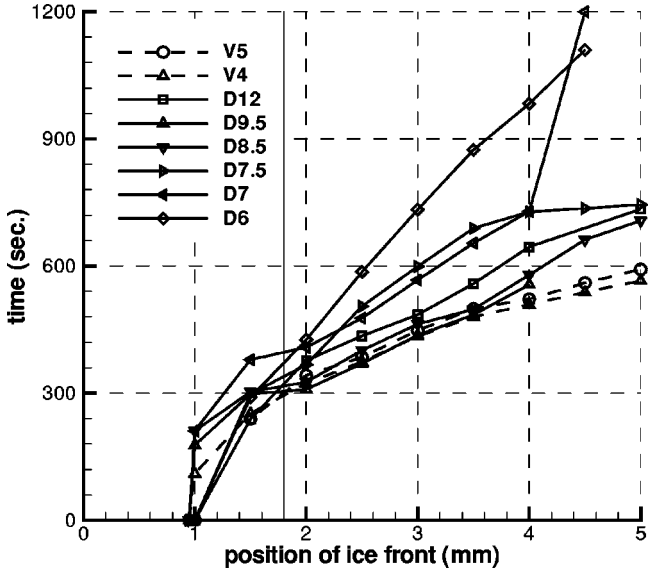

FIG. 7. The transient position of ice front tips vs time for both film and capillary freezing (case 3, $\Delta t = 28$ min). The volume of the film solution is indicated in μL following the letter "V"; the diameter of the capillary is indicated in μm following the letter "D."

dashed lines; while the data for the capillaries are represented by solid lines. A slower freezing protocol delayed the nonplanar breakdown, and produced a more flat temperature distribution in the slide. In case 2 ($\Delta t = 21$ min), the planar/nonplanar transition took place at 1.2 mm, and the critical capillary radius was about 2–5 μm. In case 3 ($\Delta t = 28$ min), the planar/nonplanar transition took place at 1.8 mm, and the critical capillary radius was about 3.5–3.8 μm. The experimental measurements for all three cases have been summarized in Table II for convenient reference.

III. HYPOTHESIS

One of the most well-known criteria for the morphological instability analysis in solidification was proposed by Mullins and Sekerka [15,19,20], which is abbreviated as "M-S" criterion in the present paper. The M-S criterion used gradients of the steady-state thermal and diffusion fields satisfying all the perturbed boundary conditions to determine the velocity of each element of the interface. Instability occurs if any Fourier component of an arbitrary perturbation grows; stability prevails if all components decay. Details can be found in Ref. [21].

Assuming the velocity of the advancing planar ice front is

TABLE II. Summary of the three test results, corresponding to different cooling rates.

Case no.	Δt (min)	x^* (mm)	$\theta_0 - \theta(x^*)$ (K)	$G(x^*)$ (K/m)	V (μm/s)	r_0 (μm)
1	14	1.0	0.5	700	5.06	7
2	21	1.2	0.7	608	6.17	2–5
3	28	1.8	1.3	512	7.70	3.5–3.8

V, the "equivalent thickness" [1] of the mass diffusion boundary layer (as we have introduced at the beginning of this paper) is estimated as $\delta = 2D_T/V$, where D_T is the solute diffusivity ($\approx 10^{-9}$ m^2/sec for most aqueous solutions with small solutes). According to the M-S criterion, instability occurs if the following function becomes positive

$$S(\omega) = -T_E \Gamma \omega^2 - \frac{\vartheta' + \vartheta}{2} + mG_c \frac{\omega^* - 2/\delta}{\omega^* - 2p/\delta}, \qquad (5)$$

where T_E is water's equilibrium temperature (i.e., 273.15 K); Γ is a capillary constant, $\Gamma = v_S \sigma_{LS}/L \approx 10^{-10}$ m for freezing of water or aqueous solutions, v_S is the specific volume of ice (m^3/kg), L is the latent heat of fusion (J/kg), σ_{LS} is the interfacial excess energy per unit area of ice-water interface (J/m^2); $\omega = 2\pi/\lambda$, and λ is the wavelength (m), $\omega^* = 1/\delta + \sqrt{1/\delta + \omega^2}$; $\vartheta = Gk_L/\bar{k}$; $\vartheta' = G'k_S/\bar{k}$, $\bar{k} = (k_S + k_L)/2$, G and G' are the thermal gradients at the unperturbed flat interface in the liquid and solid, respectively; k_S and k_L are thermal conductivities of solid and liquid, respectively; $p = 1 - k$, k is the partition coefficient, and $k \approx 10^{-8}$ [22] for most aqueous solutions with small solutes; m is the freezing point constant, $m = 1.86$ K/(mol/kg) for dilute aqueous solutions [23], G_c is the concentration gradient in the liquid at the unperturbed flat interface [mol/(kg m)].

Considering $p \approx 1$ and neglecting the difference between the thermal gradients in the liquid and solid (i.e., $G' \approx G$), the M-S criterion can be simplified to

$$S(\omega) \approx -T_E \Gamma \omega^2 - G + mG_c. \qquad (6)$$

This equation clearly indicates that the capillary effect and a positive temperature gradient are always stabilizing factors for ice growth; while the solute concentration gradient near the interface or a negative temperature gradient are always destabilizing factors. The value of $\phi = -G + mG_c$ is usually referred to as the "degree of constitutional supercooling," which must be a positive value for any perturbation to grow [1].

The concentration gradient near the interface G_c can be estimated by

$$G_c \approx \frac{c_L - c_\infty}{\frac{\delta}{2}} = \frac{c_L - c_\infty}{\frac{D_T}{V}}, \qquad (7)$$

where c_L and c_∞ are the concentrations near the interface and at the far field in the liquid, respectively. The inequality of $\phi > 0$ yields a minimum velocity that can introduce an instability, which is

$$V_0 = \frac{D_T G}{m(c_L - c_\infty)} = \frac{D_T G}{\Delta T}, \qquad (8)$$

where $\Delta T = m(c_L - c_\infty) = \theta_0 - \theta(x^*)$. Any ice front with a velocity below V_0 will remain planar.

Corresponding to $S = 0$, there is a critical wavelength λ_0 above which waves grow, below which waves decay, and at which a wave must have constant amplitude; and λ_0 is the "smallest" wavelength that can develop unstable growth. Similar to the concept of critical crystal radius that is defined in nucleation theories [3], the M-S criterion has offered a *kinetic* version of the critical size (in the format of wavelength), corresponding to certain cooling conditions, that can develop unstable growth. Since an *infinite* space was used in the derivation of the M-S criterion [15], the wavelength can assume any positive values in that problem. For ice growth in a *confined* space (the space perpendicular to the growth direction is constrained), the wavelength cannot be chosen arbitrarily, since the special solutions to the homogeneous problem have to satisfy the boundary conditions at the capillary wall (e.g., the zero mass flux condition at the capillary wall requires the concentration profile to be perpendicular to the capillary wall). In this case, the wavelength can only take *discrete* "eigenvalues," which are the fractions of the capillary radius. The perturbed interface that is most probable to develop has a wavelength of four times the capillary radius. Thus, it is further hypothesized the critical capillary radius is one quarter of the smallest wavelength; i.e.,

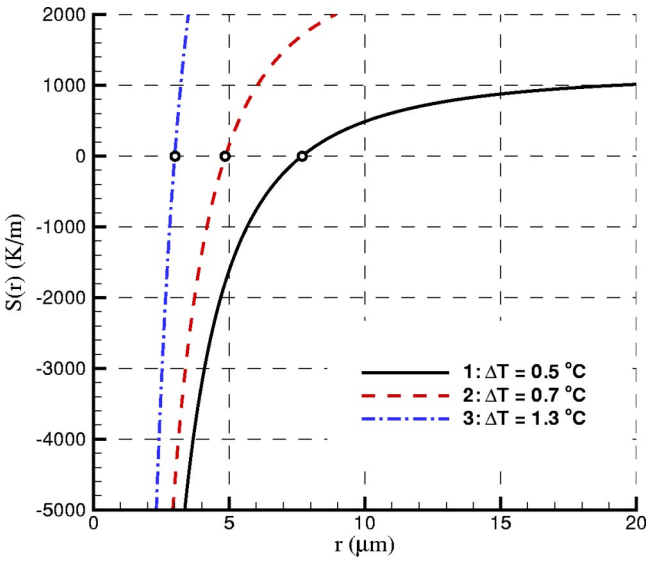

FIG. 8. Calculation of the "M-S" function $S(r)$ against the capillary radius. Case 1: $\Delta T = 0.5$ °C; case 2: $\Delta T = 0.7$ °C; and case 3: $\Delta T = 1.3$ °C.

$$r_0 = \frac{\lambda_0}{4}. \qquad (9)$$

Any capillaries with a radius less than r_0 cannot initiate unstable growth. We will examine this hypothesis against our experimental data in the following, and give some aggressive applications in cryobiology research.

A. Calculation of $S(r)$

The M-S instability function S, i.e., Eq. (5), is calculated against the capillary radius in accordance with the current experimental conditions, as shown in Fig. 8. For example, in case 1, the critical capillary radius, $r_0 = \lambda_0/4$, is calculated as 7.7 μm. This value confirms the experimental observation that at a radius of about 7 μm (see Table II), there is a change

TABLE III. The parameters used in the calculation.

Variable	Value	Unit
Γ	1.042×10^{-10}	m
D_T	1.25×10^{-9}	m^2/s
k_L	0.603	J/(s m K)
k_S	2.22	J/(s m K)
C_L	4.19×10^6	$J/(m^3K)$
C_S	1.95×10^6	$J/(m^3K)$

of the propagation velocity. This conclusion holds true for case 2 and case 3 as well. The physical parameters used in the numerical calculation are listed in Table III.

B. Calculation of $V-r_0$

Based on the M-S criterion and the current hypothesis, we can derive a relation between the ice front propagating velocity V and the critical capillary radius r_0.

Multiplying both sides of Eq. (6) with a factor of $D_T/\Delta T$ and letting $S(\omega)=0$, one has

$$0=-\frac{D_T T_E \Gamma \omega^2}{\Delta T}-\frac{D_T G}{\Delta T}+\frac{m G_c D_T}{\Delta T}. \tag{10}$$

Noting Eqs. (8) and (7), one has

$$0=-\frac{D_T T_E \Gamma \omega^2}{\Delta T}-V_0+V. \tag{11}$$

Using the current hypothesis, i.e., Eq. (9), the above equation becomes

$$0=-\frac{\pi^2}{4}\frac{D_T T_E \Gamma}{\Delta T}\frac{1}{r_0^2}-V_0+V, \tag{12}$$

which can be conveniently expressed in logarithmic coordinates, i.e.,

$$\log(V-V_0)+2\log r_0=\log\left(\frac{\pi^2}{4}\frac{D_T T_E \Gamma}{\Delta T}\right). \tag{13}$$

Still assuming the solute diffusivity $D_T\approx1.25\times10^{-9}$ m^2/s, one has a group of lines corresponding to various ΔT, as shown in Fig. 9. Note that current experimental results fall in the lines between $\Delta T=0.5$ K and $\Delta T=5$ K, which is in good agreement with the theoretical predictions. For a general physiological system, the maximum ΔT can be assumed to be 21 K, corresponding to the difference between the freezing point of water ($\theta_0=0$ °C) and the eutectic point of saline solution [$\theta(x^*)=-21$ °C]. In this sense, Fig. 9 gives a more generalized picture for capillary systems, such as biological tissues with a pore size at submicrometers. Since it is difficult to measure the velocity of ice front propagation inside tissues or organs, a differential form [24] is used to estimate the velocity from a cooling rate, i.e.,

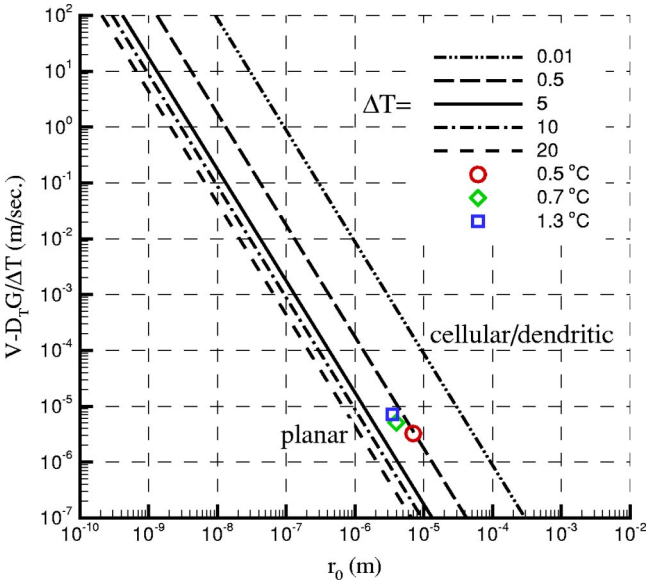

FIG. 9. The relationship between the propagating velocity and the critical capillary radius [$\Delta T=\theta_0-\theta(x^*)$].

$$B=\frac{d\theta}{dt}=\frac{d\theta}{dx}\times\frac{dx}{dt}=GV, \tag{14}$$

where B is the cooling rate, and G is the temperature gradient. In what follows, we will discuss the possible applications of Fig. 9 in cryobiology research.

1. Cryopreservation

Examine the conditions of the cartilage cryopreservation example introduced in the beginning of this paper (see Ref. [9] for details). In this case, $B\approx1$ K/min, and the minimum temperature gradient in the cartilage is assumed as (0.01 K)/(3.5 mm), where 3.5 mm is the radius of the cartilage disk. Therefore, the velocity of ice front propagation is estimated to be, at most, 350 mm/min. However, according to Fig. 9, for a 5 nm pore size [12], the minimum velocity needed to initiate unstable growth is almost 6000 mm/min. Therefore, no cellular/dendritic ice growth is expected under the experimental conditions. The ice front remains planar and the growth rate will be retarded by the diffusion of solutes.

2. Cryosurgery

It is also of great interest to examine a typical cryosurgery example and give a rough prediction of whether unstable growth can occur or not during the surgical operation. Based on a previous paper [25], we assume that a tumor has a typical dimension of 30 mm, with a temperature of −123 °C in the tumor center and 37 °C on the boundary. If the cooling rate B is 40 K/sec (near the tip of cryoprobes), one can find the critical radius: $r_0\approx30$ nm. That means if the tumor tissue has a pore size less than 60 nm, then there will be no unstable growth during the surgery.

IV. CONCLUSION AND DISCUSSION

An experiment was designed to study the radius dependence of the velocity of ice front propagation in glass capil-

laries. It was observed that there exists a critical capillary radius r_0 below which the ice growth inside slowed down; and above which the ice fronts propagated at almost the same velocity. This velocity was found comparable with that in the thin films that were sandwiched in two glass slides.

The critical radius has been related to the concept of the smallest wavelength that was used in the instability analysis of interface morphology in bulk solidification of alloys. Hypothesizing $r_0=\lambda_0/4$, it was found that the M-S criterion gives a reasonable prediction of the critical capillary radius, which has been examined in the present paper.

A logarithmic relation between the ice front propagating velocity and the critical radius [i.e., Eq. (13)] was derived and plotted in Fig. 9. This figure gives a larger view of the role of the capillary term in freezing of capillary porous systems. A future task is to develop a three-dimensional version of the chart, in terms of cooling rate, sample size, and pore size.

Of course, the validation of the present hypothesis in high-speed ice front penetration is still open. In the M-S criterion, a steady-state propagation assumption was used. This is a good approximation for alloy solidification with a larger partition coefficient *k*. However for ice, since it has almost zero solubility, most of the ice formation cases are still in the ''transient'' stage before developing a full ''steady-state'' propagation. Also, the M-S criterion was derived based on a perturbation analysis for a planar ice front. In small capillaries, the interface, even at the thermal equilibrium state, is already curved [18].

Finally, the porous structure in tissues is different from glass capillaries in its wall properties, both chemically and mechanically. Chemically, the contact angle of an ice front in a biological channel, such as a blood vessel, is assumed to be much less than 180° and might well approach 90° [26]. The contact angle might have an impact on the ice growth in capillaries. Mechanically, biological materials differ from the rigid wall of glass capillaries in that, for example, the blood vessel wall is elastic. As ice expands during phase change, there is a mechanical force applied to the wall to introduce a deformation or ''strain energy.'' This extra energy might have to be considered together with the heat transfer.

ACKNOWLEDGMENTS

This work was supported by the Whitaker Foundation, NSERC (Natural Sciences and Engineering Research Council of Canada), and Canada Research Chair Program in Interfacial Thermodynamics (J.A.W. Elliott). The authors would like to express their sincere thanks to Sherri Liang, May Chung, Simon Chi, Colleen Chan, Dr. Ayodeji Jeje, and Dr. John Matyas for their discussions and technical assistance.

[1] W. Kurz and D.J. Fisher, *Fundamentals of Solidification* (Trans Tech, Switzerland, 1984).
[2] M. Ohara and R.C. Reid, *Modeling Crystal Growth Rates from Solution* (Prentice-Hall, Englewood Cliffs, NJ, 1973).
[3] B. Chalmers, *Principles of Solidification* (Wiley, New York, 1964).
[4] K.A. Jackson and B. Chalmers, J. Appl. Phys. **29**, 1178 (1958).
[5] M.E. Glicksman, J. Cryst. Growth **42**, 347 (1977).
[6] S. Kourosh, M.E. Crawford, and K. Diller, Int. J. Heat Mass Transfer **33**, 29 (1990).
[7] S. Kourosh, K. Diller, and M. Crawford, Int. J. Heat Mass Transfer **33**, 39 (1990).
[8] K. Muldrew, M. Hurtig, K. Novak, N. Schachar, and L.E. McGann, Cryobiology **31**, 31 (1994).
[9] K. Muldrew *et al.*, Cryobiology **40**, 102 (2000).
[10] K. Muldrew *et al.*, Cryobiology **43**, 260 (2001).
[11] K. Muldrew *et al.*, Osteoarthritis Cartilage **9**, 432 (2001).
[12] A. Maroudas, *Physico-Chemical Properties of Articular Cartilage*, 2nd ed. (Pitman Medical, London, 1970), pp. 131–170.
[13] G.L. Rapatz, L.J. Menz, and B.J. Luyet, in *Cryobiology*, edited by H.T. Meryman (Academic Press, London, 1966), pp. 139–162.
[14] C. Körber and M.W. Scheiwe, J. Cryst. Growth **61**, 307 (1983).
[15] W.W. Mullins and R.F. Sekerka, J. Appl. Phys. **35**, 444 (1964).
[16] B. Rubinsky and M. Ikeda, Cryobiology **22**, 55 (1985).
[17] K.R. Diller, in *Advances in Heat Transfer*, edited by Y.I. Cho (Academic Press, San Diego, 1992), p. 184.
[18] Z. Liu, K. Muldrew, R.G. Wan, and J.A.W. Elliott, Phys. Rev. E **67**, 061602 (2003).
[19] W.W. Mullins and R.F. Sekerka, J. Appl. Phys. **34**, 323 (1963).
[20] R.F. Sekerka, J. Appl. Phys. **36**, 264 (1964).
[21] R.F. Sekerka, in *Crystal Growth: An Introduction*, edited by W. Bardsley, D.T.J. Hurle, J.B. Mullin, and P. Hartman (North-Holland, Amsterdam, Netherlands, 1973), pp. 403–443.
[22] C. Körber, M.W. Scheiwe, and K. Wollhöver, Int. J. Heat Mass Transfer **26**, 1241 (1983).
[23] R.A. Alberty and R.J. Silbey, *Physical Chemistry* (Wiley, New York, 1992).
[24] B. Rubinsky and E.G. Cravalho, Cryobiology **21**, 303 (1984).
[25] R. Wan, Z. Liu, K. Muldrew, and J. Rewcastle, Comput. Meth. Biomech. Biomed. Eng. **6**, 197 (2003).
[26] P. Mazur, in *Cryobiology*, edited by H.T. Meryman (Academic Press, London, 1966), pp. 213–315.